

Published in final edited form as:

Medchemcomm. 2013 February 1; 4(2): 443–449. doi:10.1039/C2MD20239E.

Synthesis and *in vitro* biological evaluation of pyrazole group-containing analogues for PDE10A†

Junfeng Li, Hongjun Jin, Haiying Zhou, Justin Rothfuss, and Zhude Tu

Department of Radiology, Washington University School of Medicine, St. Louis, MO, 63110, USA;

Fax: +1-314-262-8555; Tel: +1-314-362-8487

Zhude Tu: tuz@mir.wustl.edu

Abstract

Twenty eight new analogues were synthesized by optimizing the structure of **MP-10** and their *in vitro* binding affinities towards PDE10A, PDE3A/B, and PDE4A/B were determined. Among these new analogues, **10a**, **10b**, **10d**, **11a**, **11b** and **11d** are very potent towards PDE10A and have IC₅₀ values of 0.40 ± 0.02, 0.28 ± 0.06, 1.82 ± 0.25, 0.24 ± 0.05, 0.36 ± 0.03 and 1.78 ± 0.03 nM respectively; these six compounds displayed high selectivity for PDE10A *versus* PDE3A/3B/4A/4B. The promising compounds will be further validated *in vivo* to identify PDE10A imaging tracers.

Introduction

Phosphodiesterase 10A (PDE10A) is one of the 11 families of phosphodiesterase enzymes. PDE10A is a unique dual specificity enzyme; it is able to hydrolyze cyclic adenosine monophosphate (cAMP) and cyclic guanosine monophosphate (cGMP) to inactive adenosine monophosphate (AMP) and guanosine monophosphate GMP, respectively.^{1,2} PDE10A was identified independently by three groups in 1999 (ref. 2–4) and has the most unique expression with mRNA levels in the brain and testis.³ Within the brain, the highest expression of PDE10A protein is in the medium spiny neurons of the striatum (caudate and putamen), nucleus accumbens, and olfactory tubercle of mice, dogs, cynomolgus and humans.⁵ Due to the unique striatal localization of PDE10A and the function of PDE10A in the brain, inhibition of PDE10A represents a novel approach for treating neurological and psychiatric disorders such as schizophrenia, Parkinson's disease, and Huntington's disease (HD);^{6–8} this therapeutic approach may avoid unwanted side effects such as extrapyramidal symptoms of conventional therapeutics. For example, investigating the levels of PDE10A in the brain of patients with Huntington's disease indicated that the level of PDE10A protein was decreased compared to that of age-matched healthy individuals;⁹ after treating with PDE10A inhibitor, 2-[4-[pyridin-4-yl]-1-(2,2,2-trifluoroethyl)-1*H*-pyrazol-3-yl]-phenoxy-methyl]-quinoline (**TP-10**), an analogue of 2-((4-(1-methyl-4-(pyridin-4-yl)-1*H*-pyrazol-3-yl)phenoxy)-methyl)quinoline (**MP-10**) (Fig. 1), both neuropathology and symptoms in R6/2 mice were ameliorated; the behavioural symptoms of R6/2 mice, such as rotarod performance, were improved.¹⁰ In addition, chronically treating with **TP-10** resulted in changes in gene expression¹¹ in the striatum of engineered PDE10A knocked out mice; this provided more evidence that the PDE10A enzyme is a promising therapeutic target for psychotic and related neurodegenerative diseases.

†Electronic supplementary information (ESI) available. See DOI: 10.1039/c2md20239e

Correspondence to: Zhude Tu, tuz@mir.wustl.edu.

Positron emission tomography (PET) provides a unique and novel non-invasive imaging tool to investigate the changes in levels of PDE10A in the brain of living subjects and to study the physiological function of PDE10A in the central nervous system (CNS). Investigators have made significant efforts to identify a clinically suitable PET probe for imaging the changes in levels of PDE10A in the human brain.^{8,12–14} In recent years, [¹¹C]-papaverine and other radioligands were evaluated *in vivo*.^{15–20} However, due to the lack of suitable radiopharmaceutical properties of the reported radiotracers,^{15–20} the evaluation of PDE10A PET tracers is still in process. To date, no clinically suitable PET tracer was reported. Among the reported PET radiotracers, substituted pyrazole-containing ligands radio-labeled by introducing carbon-11, or fluorine-18 *via* *N*-alkylation of the pyrazole ring had attracted more attention^{16,18,19} because of the use of **MP-10** as a PDE10A inhibitor in clinical trials for treatment of schizophrenia;²¹ PET radiotracers, [¹¹C]**MP-10**, ¹⁸F-JNJ41510417, [¹⁸F]**1**, [¹⁸F]**2** shown in Fig. 1, were made by introducing the [¹¹C]methyl, [¹⁸F]fluoroethyl or [¹⁸F]fluoropropyl group on the *N*-atom of the pyrazole scaffold and further evaluated *in vivo* in rodents and monkeys.^{16,18,19,22} Our group had reported that the *in vivo* microPET studies of [¹¹C] **MP-10** in monkeys showed a very clear anatomic structure of monkey brain and the highest accumulation of radioactivity in the striatal area of the brain, higher target-to-non-target ratios, but the kinetics displayed an increasing trend post-injection of [¹¹C]**MP-10**. Further metabolite analysis of monkey plasma, rodent plasma and brain tissues revealed that the radioactive metabolite formed post-injection of radiotracer [¹¹C]**MP-10** by *O*-dealkylation of [¹¹C]**MP-10** *in vivo*; this radioactive metabolite was able to cross the blood–brain-barrier and accumulate in the brain; radioactivity of the radioactive metabolite in the brain may lead to misinterpretation of the measurement of PDE10A levels in the brain. Thus, further optimization of the pyrazole-containing analogues to overcome the radioactive metabolite concern is imperative.

In our current studies, we had taken the following strategies to design the new analogues to overcome the radioactive metabolite concern: (1) introducing a methoxy into a quinoline fragment of the **MP-10** structure, which creates a new position to label with carbon-11; we expect that the new radioactive metabolite obtained from the substituted 2-methylquinoline fragment *via* *O*-dealkylation of phenyl ether does not have the capability to cross the blood–brain-barrier (BBB) and enter into the brain; (2) replacing the oxygen (O) atom that links the substituted methyl-quinoline fragment and the substituted pyrazole fragment of **MP-10** with a nitrogen (N) or sulfur (S) atom; we expect that the new derivatives in which the N or S serves as a linkage atom will be more stable. This may increase the metabolic stability of radiotracers *in vivo* or form new radioactive metabolites that do not enter into the brain and accumulate in the striatal area and other regions. In the current manuscript, we reported our efforts on synthesizing the new analogues based on the above design strategies and their *in vitro* binding affinity evaluation.

Results and discussion

Chemistry

The syntheses of compounds **10a–f** and **11a–f** were accomplished according to Scheme 1.

The syntheses of several **MP-10** analogues were achieved by a Mitsunobu reaction of heteroaromatic benzyl alcohols with **6** as an alkylating agent.²¹ Attempts to synthesize compounds **10a–f** and **11a–f** were very challenging due to similar retention factor values (*R_f*) of intermediates quinolin-2-yl-methanol and the final compounds **10a–f** and **11a–f**. To overcome this challenge, an alternative approach was taken; substituted phenols **6** or **7** were coupled with substituted 2-bromomethylquinolines **9a–f** to afford target compounds for which the purification was easily achieved by column chromatography. Synthesis of target compounds began with commercially available 4-(benzyloxy) benzoic acid (**3**). Following

the literature procedure,²¹ compounds **4** and **5** were afforded in three steps. Debenzylation of compounds **4** and **5** afforded substituted phenols **6** and **7**. Commercially unavailable 4-methoxy-2-methylquinoline (**8b**) was synthesized by treating 4-chlorine-2-methylquinoline with sodium methoxide (NaOCH₃);^{23,24} 8-methoxy-2-methylquinoline (**8f**) was synthesized *via* *O*-alkylation of 2-methylquinolin-8-ol with iodomethane in dimethylformamide (DMF). Methoxy-2-bromomethylquinolines **9a–f** were synthesized by bromination of methoxy substituted 2-methylquinolines **8a–f** using *N*-bromosuccinimide (NBS). *O*-Alkylation of phenols **6** or **7** with substituted 2-bromomethylquinolines **9a–f** afforded compounds **10a–f** or **11a–f** respectively, following the literature procedure with minor modification.^{21,25}

The syntheses of the S-atom bridged analogues **10g–j** and **11g–j** were achieved according to Scheme 2. Synthesis began by reacting 4-bromobenzoic acid **12** with *N,O*-dimethylhydroxylamine hydrochloride and 1,1-carbonyldiimidazole (CDI) to afford Weinreb amide **13** in nearly quantitative yield. Treatment of 4-picoline with lithium diisopropyl amide (LDA) at –78 °C followed by adding this solution to the solution of **13** in tetrahydrofuran (THF) afforded compound **14**. Treatment of compound **14** with dimethoxymethyl-dimethyl amine afforded the key intermediate enaminones **15** and **16**. Compounds **15** or **16** upon treatment with sodium thiomethoxide in dimethylacetamide (DMA) at high temperature afforded intermediates **17** or **18** respectively. Coupling of thiophenols **17** or **18** with substituted 2-bromomethylquinolines **9b, 9d–f** afforded thioether analogues **10g–j** or **11g–j**.

The syntheses of the N-atom bridged analogues **10k–n** and **11k–n** were achieved according to Scheme 3. The Gabriel synthesis procedure^{26–28} was followed by treating the aromatic bromides **15** or **16** with potassium phthalimide to afford the corresponding *N*-alkylphthalimide **19** or **21**. Treating **19** or **21** with ethanolic hydrazine following the Ing–Manske procedure²⁹ afforded aromatic amines **20** or **22**. *N*-Alkylation of the aromatic amines **20** or **22** with substituted 2-bromomethylquinolines **9b, 9d–f** afforded the desired N-atom bridged analogues **10k–n** or **11k–n**.

Biological binding studies

We explored the structure of **MP-10** by introducing the methoxy group into the quinoline fragment of the **MP-10**. The strategy of introducing the methoxy group is to provide a new position for introducing the [¹¹C]methoxy group if the new analogues have high binding affinity and selectivity for PDE10A. To test this strategy, we first synthesized compounds **10b, 10d–f** and their regioisomers **11b, 11d–f** by introducing the methoxy group at the 4, 6, 7 and 8 positions of the quinoline fragment. The *in vitro* PDE10A binding affinity data of compounds **10b, 10d–f** displayed the decreasing order as: 4-methoxy > 6-methoxy > 7-methoxy ≈ 8-methoxy; the IC₅₀ values (nM) of **10b** and **10d–f** were 0.28 ± 0.06, 1.82 ± 0.25, 46.0 ± 6, and 41.5 ± 6.5 nM respectively. Among compounds **10b, 10d–f**, compounds **10b** and **10d** are very potent for PDE10A, particularly, for **10b**, the *in vitro* IC₅₀ value reached 0.28 nM.

To extend our structural modification studies, the regioisomeric counterparts **11b, 11d–f** were also synthesized and their *in vitro* binding affinities were determined as shown in Table 1. The *in vitro* data suggested that compounds **11b, 11d–f** and compounds **10b, 10d–f** have similar decreasing binding affinity order; for compounds **11b, 11d, 11e**, and **11f**, the IC₅₀ values (nM) were 0.36 ± 0.03, 1.78 ± 0.03, 95 ± 15, and 199 ± 21 nM; 4-methoxy substituted compound **11b**, similar to its counterpart **10b**, has the highest binding affinity for PDE10A. The next most potent compound is the 6-methoxy substituted **11d**. Compounds **10b** and **11b** had similar subnanomolar affinities (0.1 nM < IC₅₀ values < 0.5 nM). However, for the less potent compounds **11e** and **11f**, the IC₅₀ values revealed that the 8-

methoxy substituted **11f** (199 nM) has a 2-fold higher IC₅₀ value than that the 7-methoxy substituted compound **11e** (95 nM).

From the above structure–activity relationship analysis, we concluded that introduction of a methoxy group at an appropriate position of the quinoline fragment in the structure of **MP-10** was able to retain the high PDE10A binding affinity. Thus, we further explored the structure of **MP-10** by replacement of the O-atom link bridge with a N-atom or S-atom. For the S-atom bridged analogues, compounds **10g–j** and **11g–j** were synthesized; for the N-atom bridged analogues, **10k–n** and **11k–n** were synthesized. Our *in vitro* data revealed: (1) compounds **10g–j**, containing a 4-(1-methyl-4-(pyridin-4-yl)-1*H*-pyrazol-5-yl)phenyl fragment, had higher affinity than their corresponding isomers **11g–j**, containing a 4-(1-methyl-4-(pyridin-4-yl)-1*H*-pyrazol-3-yl)phenyl fragment; this observation was similar to the results of the O-atom bridged analogues **10b**, **10d–f** versus **11b**, **11d–f**; (2) even the S-atom bridged analogues **10g–j** displayed higher binding affinity than that N-atom bridged analogues **10k–n**, and the binding affinity of methoxy substituted analogues displayed the order as: 4-methoxy > 6-methoxy ≈ 7-methoxy > 8-methoxy, for which the IC₅₀ values are 168 ± 52, 415 ± 65, 400 ± 60, 635 ± 15 nM for compounds **10g–j** respectively. The PDE10A binding affinities of S-atom bridged analogues **10g–j** were much lower than those of their corresponding O-atom bridged analogues **10b**, **10d–f**. Among 16 compounds **10g–n** and **11g–n** containing either S-atom or N-atom bridge, the most potent compound **10g** had the IC₅₀ value of 168 ± 52 nM, which was 600-fold less potent than that of **10b** (0.28 ± 0.06 nM), the corresponding O-atom bridged analogue. The binding affinities of N-atom link bridge analogues **10k–n** and **11k–n** decreased dramatically (IC₅₀ value > 645 nM). Thus, replacing the O-atom bridge linkage with a S-atom or N-atom did not generate PDE10A potent compounds.

Based on above *in vitro* data, only the O-atom bridge linkage was able to retain the high binding potency for the PDE10A enzyme. We further synthesized **10a**, **10c**, **11a**, and **11c** by introducing the methoxy group at 3 and 5 positions of the quinoline fragment; the *in vitro* data suggested that 3-methoxy substituted compounds **10a** and **11a** were very potent for PDE10A and the IC₅₀ values are 0.40 ± 0.02 and 0.24 ± 0.05 nM, which had similar PDE10A binding potency to that of the 4-methoxy substituted compounds, **10b** and **11b**. However, 5-methoxy substituted compounds **10c** and **11c** displayed lower PDE10A binding affinities; the IC₅₀ values were 60 ± 26 nM for **10c** and 81.4 ± 9.2 nM for **11c**.

Inhibition of PDE3A/B could lead to arrhythmia and increased mortality,^{30,31} and the role of phosphodiesterase 4 could be a regulator of central nervous system function and inhibition of PDE4A could increase heart and respiratory rates.³² The binding affinities of compounds **10a**, **10b**, **10d**, **11a**, **11b**, and **11d**, which have IC₅₀ values less than 5 nM for PDE10A, were further evaluated *in vitro* for PDE3A/B and PDE4A/B; the results are shown in Table 2. The *in vitro* data suggested that these six compounds had very weak binding affinity for PDE3A/3B and PDE4A/4B with the IC₅₀ value > 1500 nM. This suggested that six compounds **10a**, **10b**, **10d**, **11a**, **11b** and **11d** not only had high potency for PDE10A but also had high selectivity for PDE10A versus PDE3A/3B and 4A/4B.

Conclusion

In the present study, we optimized the structure of **MP-10** to identify new compounds by introducing a methoxy group in the quinoline fragment. The *in vitro* data suggested that six compounds **10a**, **10b**, **10d**, **11a**, **11b**, and **11d** had high PDE10 binding potency with IC₅₀ values of 0.40 ± 0.02, 0.28 ± 0.06, 1.82 ± 0.25, 0.24 ± 0.05, 0.36 ± 0.03, and 1.78 ± 0.03 nM respectively. These six compounds also displayed high selectivity for PDE10A against PDE3A/3B and PDE4A/4B with IC₅₀ > 1500 nM. After further evaluating their PDE10A

binding selectivity against another PDE enzyme family, it is worthwhile to label them with carbon-11 to conduct further *in vivo* validation. However, optimizing the structure of **MP-10** by replacing the O-atom bridge with a S-atom or N-atom and introducing the methoxy group into the quinoline fragment led to a dramatic loss of the PDE10A binding affinities for the newly synthesized analogues. These new analogues and their *in vitro* binding affinities could provide helpful information for further structure– activity relationship studies.

Supplementary Material

Refer to Web version on PubMed Central for supplementary material.

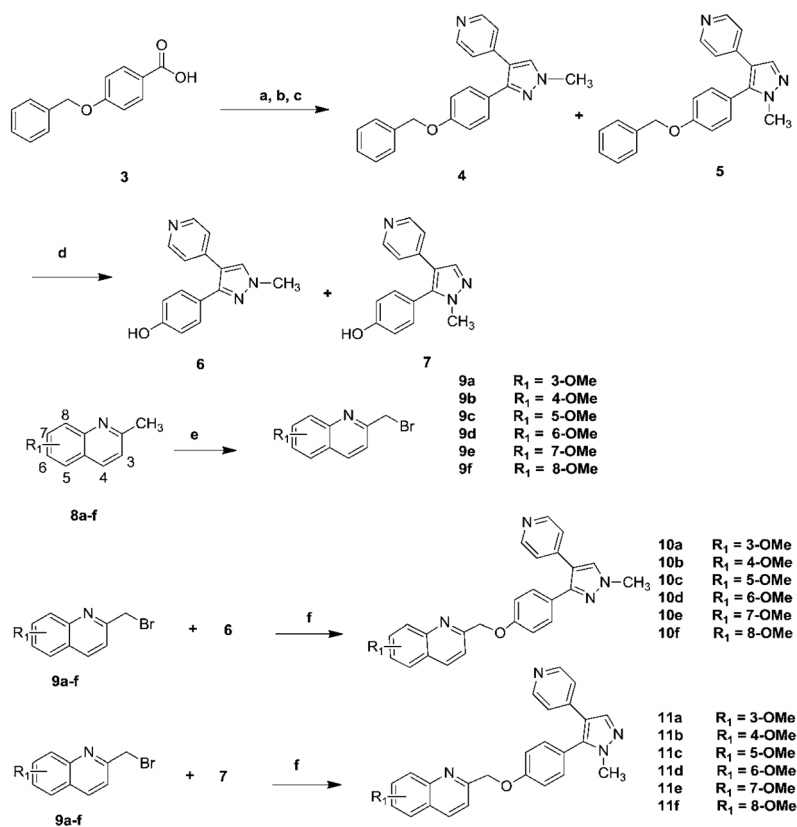
Abbreviations

Anal	Analysis
BBB	Blood–brain-barrier
CDI	1,1-Carbonyldiimidazole
CNS	Central nervous system
cAMP	cyclic Adenosine monophosphate
cGMP	cyclic Guanosine monophosphate
DCM	Dichloromethane
DMF	<i>N,N</i> -Dimethylformamide
EtOH	Ethanol
EtOAc	Ethyl acetate
HD	Huntington’s disease
LDA	Lithium diisopropyl amide
MeOH	Methanol
MP-10	2-((4-(1-Methyl-4-(pyridin-4-yl)-1 <i>H</i> -pyrazol-3-yl)-phenoxy)-methyl)quinolone
NBS	<i>N</i> -Bromosuccinimide
PDE3A	Phosphodiesterase 3A
PDE3B	Phosphodiesterase 3B
PDE4A	Phosphodiesterase 4A
PDE4B	Phosphodiesterase 4B
PDE10A	Phosphodiesterase 10A
PET	Positron emission tomography
NaOCH₃	Sodium methoxide
THF	Tetrahydrofuran
TEA	Triethylamine
TP-10	2-[4-[Pyridin-4-yl-1-(2,2,2-trifluoro-ethyl)-1 <i>H</i> -pyrazol-3-yl]-phoxymethyl]-quinoline

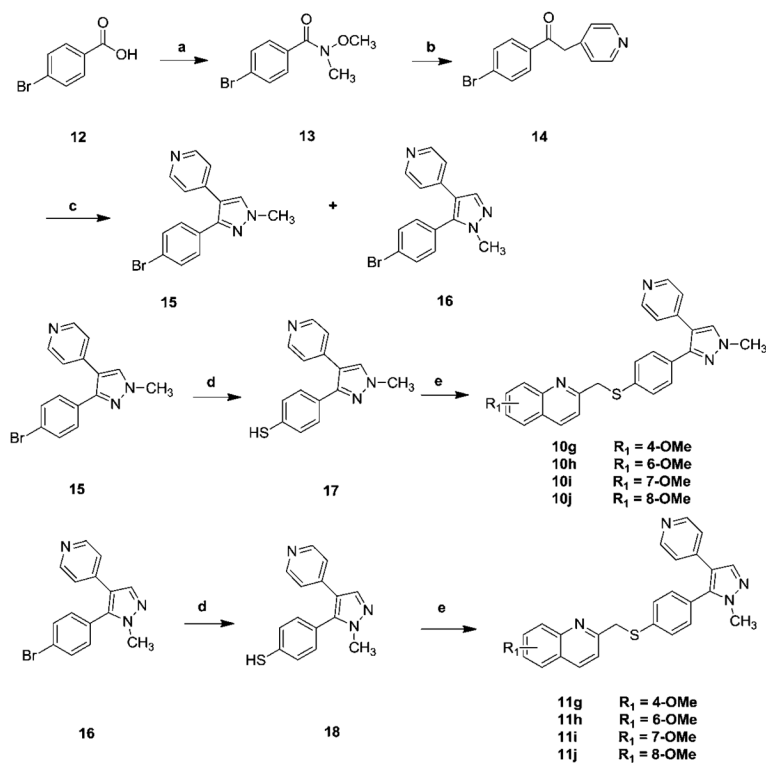
References

1. Bora RS, Gupta D, Malik R, Chachra S, Sharma P, Saini KS. *Biotechnol Appl Biochem*. 2008; 49:129–134. [PubMed: 17640173]
2. Loughney K, Snyder PB, Uher L, Rosman GJ, Ferguson K, Florio VA. *Gene*. 1999; 234:109–117. [PubMed: 10393245]
3. Soderling SH, Bayuga SJ, Beavo JA. *Proc Natl Acad Sci U S A*. 1999; 96:7071–7076. [PubMed: 10359840]
4. Fujishige K, Kotera J, Michibata H, Yuasa K, Takebayashi S, Okumura K, Omori K. *J Biol Chem*. 1999; 274:18438–18445. [PubMed: 10373451]
5. Coskran TM, Morton D, Menniti FS, Adamowicz WO, Kleiman RJ, Ryan AM, Strick CA, Schmidt CJ, Stephenson DT. *J Histochem Cytochem*. 2006; 54:1205–1213. [PubMed: 16864896]
6. Menniti FS, Faraci WS, Schmidt CJ. *Nat Rev Drug Discovery*. 2006; 5:660–670.
7. Menniti FS, Chappie TA, Humphrey JM, Schmidt CJ. *Curr Opin Invest Drugs*. 2007; 8:54–59.
8. Siuciak JA. *CNS Drugs*. 2008; 22:983–993. [PubMed: 18998737]
9. Hebb AL, Robertson HA, Denovan-Wright EM. *Neuroscience*. 2004; 123:967–981. [PubMed: 14751289]
10. Giampa C, Laurenti D, Anzilotti S, Bernardi G, Menniti FS, Fusco FR. *PLoS One*. 2010; 5:e13417. [PubMed: 20976216]
11. Kleiman RJ, Kimmel LH, Bove SE, Lanz TA, Harms JF, Romegialli A, Miller KS, Willis A, des Etages S, Kuhn M, Schmidt CJ. *J Pharmacol Exp Ther*. 2011; 336:64–76. [PubMed: 20923867]
12. Siuciak JA, Strick CA. *Expert Opin Drug Discovery*. 2007; 2:1001–1009.
13. Kehler J, Ritzen A, Greve DR. *Expert Opin Ther Pat*. 2007; 17:147–158.
14. Kehler J, Kilburn JP. *Expert Opin Ther Pat*. 2009; 19:1715–1725. [PubMed: 19939189]
15. Tu Z, Xu J, Jones LA, Li S, Mach RH. *Nucl Med Biol*. 2010; 37:509–516. [PubMed: 20447563]
16. Tu Z, Fan J, Li S, Jones LA, Cui J, Padakanti PK, Xu J, Zeng D, Shoghi KI, Perlmutter JS, Mach RH. *Bioorg Med Chem*. 2011; 19:1666–1673. [PubMed: 21315609]
17. Zhang Z, Lu X, Xu J, Rothfuss J, Mach RH, Tu Z. *Eur J Med Chem*. 2011; 46:3986–3995. [PubMed: 21705115]
18. Celen S, Koole M, De Angelis M, Sannen I, Chitneni SK, Alcazar J, Dedeurwaerdere S, Moechars D, Schmidt M, Verbruggen A, Langlois X, Van Laere K, Andres JI, Bormans G. *J Nucl Med*. 2010; 51:1584–1591. [PubMed: 20847170]
19. Plisson C, Salinas C, Weinzimmer D, Labaree D, Lin SF, Ding YS, Jakobsen S, Smith PW, Eiji K, Carson RE, Gunn RN, Rabiner EA. *Nucl Med Biol*. 2011; 38:875–884. [PubMed: 21843784]
20. Hu E, Ma J, Biorn C, Lester-Zeiner D, Cho R, Rumpfelt S, Kunz RK, Nixey T, Michelsen K, Miller S, Shi J, Wong J, Hill Della Puppa G, Able J, Talreja S, Hwang DR, Hitchcock SA, Porter A, Immke D, Allen JR, Treanor J, Chen H. *J Med Chem*. 2012; 55:4776–4787. [PubMed: 22548439]
21. Verhoest PR, Chapin DS, Corman M, Fonseca K, Harms JF, Hou XJ, Marr ES, Menniti FS, Nelson F, O'Connor R, Pandit J, Proulx-LaFrance C, Schmidt AW, Schmidt CJ, Suiciak JA, Liras S. *J Med Chem*. 2009; 52:5188–5196. [PubMed: 19630403]
22. Andrés JI, de Angelis M, Alcázar J, Celen S, Bormans G. *Curr Top Med Chem*. 2012; 12:1224–1236. [PubMed: 22571785]
23. Lister T, Prager RH, Tsacomas M, Wilkinson KL. *Aust J Chem*. 2003; 56:913–916.
24. Andersen KE, Lundt BF, Jorgensen AS, Braestrup C. *Eur J Med Chem*. 1996; 31:417–425.
25. Tu Z, Fan J, Li S, Jones LA, Cui J, Padakanti PK, Xu J, Zeng D, Shoghi KI, Perlmutter JS, Mach RH. *Bioorg Med Chem*. 2011; 19:1666–1673. [PubMed: 21315609]
26. Sheehan JC, Bolhofer VA. *J Am Chem Soc*. 1950; 72:2786.
27. Khan MN. *J Org Chem*. 1996; 61:8063–8068. [PubMed: 11667789]
28. Landini D, Rolla F. *Synthesis*. 1976:389–391.
29. Ing HR, Manske RHF. *J Chem Soc*. 1926:2348–2351.
30. Mager G, Klocke RK, Kux A, Hopp HW, Hilger HH. *Am Heart J*. 1991; 121:1974–1983. [PubMed: 1852090]

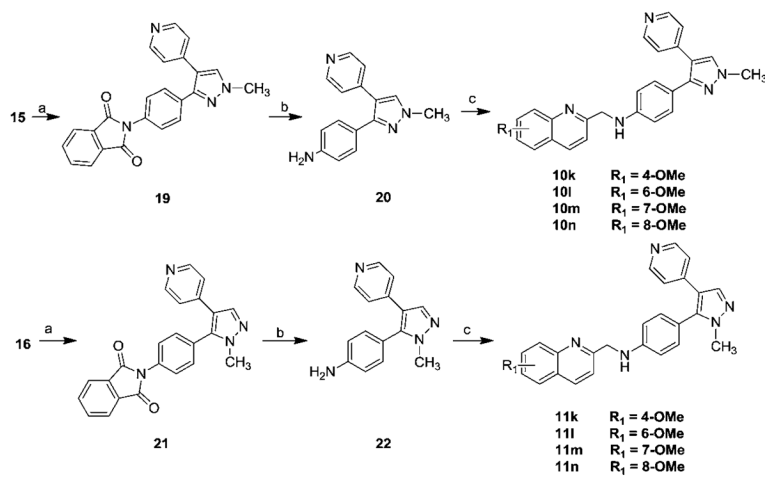
31. Movsesian M, Stehlik J, Vandeput F, Bristow MR. Heart Fail Rev. 2009; 14:255–263. [PubMed: 19096931]
32. Heaslip RJ, Evans DY. Eur J Pharmacol. 1995; 286:281–290. [PubMed: 8608790]

**Scheme 1.**

Synthesis of compounds **10a–f** and **11a–f**. *Reagents and conditions*: (a) CDI, *N,N*-dimethylhydroxylamine hydrochloride, NEt_3 , CH_2Cl_2 , rt; (b) 4-picoline, LDA, -78 C to rt; (c) *N,N*-dimethylformamide-dimethyl acetal, reflux, then methylhydrazine; (d) H_2 , Pd/C, ethanol/EtOAc; (e) NBS, AIBN, CCl_4 , reflux; (f) NaH, DMF, rt.

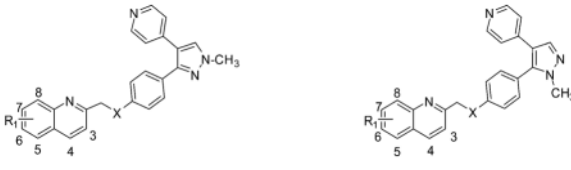
**Scheme 2.**

Synthesis of compounds **10g–j** and **11g–j**. *Reagents and conditions*: (a) CDI, *N,O*-dimethylhydroxylamine hydrochloride, NEt_3 , CH_2Cl_2 , rt; (b) 4-picoline, LDA, -78°C to rt; (c) *N,N*-dimethylformamide-dimethyl acetal, reflux, then NH_2NHCH_3 ; (d) NaSMe , DMA, 150°C ; (e) substituted 2-bromomethylquinoline, NaH , DMF, 0°C to rt, overnight.

**Scheme 3.**

Synthesis of compounds **10k–n** and **11k–n**. *Reagents and conditions:* (a) potassium phthalimide, CuI, DMA, 150 °C; (b) hydrazine hydrate, EtOH, reflux; (c) substituted 2-bromomethylquinoline, Na₂CO₃, acetonitrile, 80 °C.

Table 1

PDE10A affinities of new analogues^a


Compd	X	R1	IC ₅₀ value (nM)	
			PDE10A	Log Db
10a	O	3-OMe	0.40 ± 0.02	3.87
10b	O	4-OMe	0.28 ± 0.06	3.79
10c	O	5-OMe	60 ± 26	3.92
10d	O	6-OMe	1.82 ± 0.25	3.61
10e	O	7-OMe	46 ± 6	3.77
10f	O	8-OMe	41.5 ± 6.5	3.28
10g	S	4-OMe	168 ± 52	3.89
10h	S	6-OMe	415 ± 65	3.72
10i	S	7-OMe	400 ± 60	3.88
10j	S	8-OMe	635 ± 15	3.39
10k	N	4-OMe	13 900 ± 1100	3.52
10l	N	6-OMe	7500 ± 700	3.36
10m	N	7-OMe	7400 ± 600	3.52
10n	N	8-OMe	10 900 ± 700	3.02
11a	O	3-OMe	0.24 ± 0.05	3.87
11b	O	4-OMe	0.36 ± 0.03	3.79
11c	O	5-OMe	81.4 ± 9.2	3.92
11d	O	6-OMe	1.78 ± 0.03	3.61
11e	O	7-OMe	95 ± 15	3.77
11f	O	8-OMe	199 ± 21	3.28
11g	S	4-OMe	1850 ± 450	3.89
11h	S	6-OMe	610 ± 80	3.72
11i	S	7-OMe	635 ± 55	3.88
11j	S	8-OMe	3050 ± 450	3.39
11k	N	4-OMe	645 ± 255	3.52
11l	N	6-OMe	4250 ± 650	3.36
11m	N	7-OMe	5150 ± 250	3.52
11n	N	8-OMe	4600 ± 400	3.02

^aIC₅₀ is defined as the concentration of the inhibitor required to reduce the [³H]cAMP hydrolysis activity of recombinant human PED10A by 50% with scintillation proximity assay.

^bCalculated value at pH = 7.4 by ACD/I-Lab ver. 7.0 (Advanced Chemistry Development, Inc., Canada).

Table 2

PDE3A/B and PDE4A/B affinities of lead analogues

Compd	IC ₅₀ value (10 ³ × nM)			
	PDE3A	PDE3B	PDE4A	PDE4B
10a	123 ± 21	82.7 ± 10	3.85 ± 0.23	3.43 ± 0.21
10b	27.5 ± 2.5	3.85 ± 0.95	2.56 ± 0.11	1.79 ± 0.10
10d	78.0 ± 4.0	9.75 ± 1.25	3.37 ± 0.18	2.56 ± 0.09
11a	18.7 ± 3.1	16.9 ± 2.1	199 ± 16.0	31.5 ± 3.60
11b	29.0 ± 4.0	4.80 ± 1.20	4.18 ± 0.33	5.06 ± 0.40
11d	1.50 ± 0.50	3.00 ± 0.14	5.60 ± 0.52	7.10 ± 0.58